Int J Adv Manuf Technol (2017) 92:831–838
DOI 10.1007/s00170-017-0169-5

ORIGINAL ARTICLE

Development of high efficiency infrared-heating-assisted micro-injection molding for fabricating micro-needle array

Shan Gao[1] · **Zhongjun Qiu**[1] · **Zhuang Ma**[1] · **Yujun Yang**[2]

Received: 9 October 2016 / Accepted: 15 February 2017 / Published online: 6 March 2017

Abstract Micro-injection molding (μIM) is considered to be an important method for fabricating micro-needle array which is widely researched in recent years, and mold temperature is one of the important factors that affect the mold filling quality of the polymer melt during the micro-injection molding. In this paper, an infrared heating method is adopted to raise the mold temperature rapidly for improving molding quality of micro-needle array. According to the simulation of the reflector type, which has an important effect on the efficiency of infrared heating system, an infrared heating system with high efficiency is developed and used in the developed infrared-heating-assisted μIM system. A series of verification experiments are carried out to verify the feasibility and the heating effect of the developed system. The experimental results show that the developed infrared heating system can achieve high efficiency and uniform heating of mold surface and the infrared-heating-assisted μIM process for fabricating micro-needle array can improve mold filling capability of the polymer melt and optimize the replication quality (filling height, uniformity, and shrinkage) of parts.

Keywords Micro-injection molding · Micro-needle array · Infrared heating · Mold temperature

✉ Zhongjun Qiu
qiuzhongjun@tju.edu.cn

[1] State Key Laboratory of Precision Measuring Technology & Instruments, Tianjin University, 92 Weijin Road, Tianjin 300072, China

[2] Guangdong Flory-Tech Ltd, Huizhou 516001, China

1 Introduction

Micro-needle array is widely used in the fields of medicine [1–4], micro-electromechanical systems [5–7], biology [8–10], and some others. Micro-injection molding (μIM) is an important method for the production of micro-needle array because of its low manufacturing cost, short production cycle, mass production, good repeatability and simple process, etc. [11–13]. However, the mold filling condition of the traditional injection molding technology is not suitable for the molding of plastic parts with micro-structures, such as micro-needle array with high aspect ratio [14, 15]. This is because the rapidly decreasing melt temperature and increasing melt viscosity, which are caused by the rapid heat dissipation in the micro-cavity with small size and large surface-volume ratio, would worsen the filling quality. More importantly, for micro-structure with high aspect ratio, the frozen layer generated during the melt contact with the cavity wall will also hinder the melt filling [16, 17].

To improve this problem, raising the mold temperature has been shown in many studies to be a very effective measure [18, 19]. Various heating methods, such as induction heating [20], flame heating [21], electric heating [22], steam heating [23], infrared heating [24], etc., have been proposed for rapidly increasing the mold temperature. The infrared heating method is the focus of attention for rapidly increasing the mold temperature because of the advantages of energy saving, clean, safe, belongs to external heating mode, and does not substantially change the mold system [24].

Infrared heating is a form of radiation that resembles and behaves like light rays. By exposing an object to infrared radiation (wavelength of 0.78 to 1000 μm), the heat energy absorbed by the object can achieve rapid heating, drying, dehydration, baking and curing functions, etc. Some researchers have considered using infrared heating to raise the mold

temperature in injection molding. Chang et al. [25] designed and investigated an infrared rapid surface heating system for injection molding. The rapid heating ability of the infrared heating system was confirmed on the mold plate by thermal video system. The enhanced filling ability due to rapid heating of mold surface was clarified by the results of modified spiral flow and microprobe injection molding. Saito et al. [26] proposed an innovative infrared-radiation-heating-assisted injection molding process and investigated the effect of radiation heating by mathematical simulation and experiment, respectively. The results can be concluded that the proposed technique is appropriate for processes that require a high added value for the molded products. Yu et al. [27] also designed an infrared heating system used in μIM and raised the mold cavity temperature locally to facilitate the replication of the micro-structure. However, in-depth investigations about the energy conversion efficiency and heating mechanism are lacking. Also, the applicability of the infrared-heating-assisted micro-injection molding method for manufacturing the micro-plastic part with high aspect ratio structures, such as micro-needle array, has not yet been clarified.

In this paper, an infrared-heating-assisted μIM system for fabricating micro-needle array is developed using a designed infrared heating device with high efficiency. The infrared heating device is built based on the numerical simulation and mechanism analysis of the heating efficiency within the selection of different reflector types. The validity of the designed device is verified by the analysis and discussion of a heating experiment on a steel block. Using the designed infrared heating device, a micro-needle array injection molding experiment is carried out. According to the analysis of the height and shrinkage performance of micro-needles, the feasibility of the infrared-heating-assisted μIM method for fabricating micro-needle array is discussed and verified, and the improvement of micro-needle array molding quality by the developed system is clarified.

2 Materials and methods

2.1 Infrared-heating-assisted μIM system

An infrared-heating-assisted μIM system principle diagram is shown in Fig. 1. An infrared heating device is added into an injection molding machine for heating the moving mold and stationary mold at the same time during the μIM process, and efficiently raises the mold temperature rapidly just before the mold-closing. A temperature sensor is put into the insert just beside the cavity for measuring the real-time temperature of the mold surface. An infrared heating controller is put into the machine for dealing the temperature feedback from the sensor and controlling the driving motor of infrared heating device. The infrared heating device, temperature sensor, and infrared heating controller form a complete closed-loop infrared heating system which is controlled by the industrial personal computer and form a linkage with the motion of micro-injection molding.

At the beginning of the μIM process, the industrial personal computer gives a signal to the infrared heating controller which controls the driving motor to drive the infrared heating device moving down from home position to the position that aims to the surface of insert, and then the infrared heating lamps turn on to heat the inserts on both sides. The real-time temperature of the insert is measured by a temperature sensor and given to the infrared heating controller. When the set temperature threshold is reached, the infrared heating device which is controlled by the infrared heating controller will turn off the lamps and move up from the injection molding area. After the infrared heating device returns to the home position, the infrared heating controller will feed back a signal to the industrial personal computer and the mold-closing immediately begins as the beginning of a normal μIM process.

2.2 Molding material

In this study, polypropylene (PP), which is a common thermoplastic resin with low melt viscosity and good fluidity, is employed to fabricate micro-needle array. The melt flow rate of the material is 60 g/10 min, the density is 0.9 g/cm^3, and the molding shrinkage is 1.2%. The material is preconditioned for 2 h with a dryer at 80 °C before injection molding.

2.3 Process parameters

An injection molding machine (FANUC ROBOSHOT S-2000*i* 50B), which is an all-electric injection molding machine, was utilized to conduct the infrared-heating-assisted μIM experiment of micro-needle array. μIM parameters, which have great influence on the product quality, are shown in Table 1. As a workpiece, micro-needle array is formed by eight micro-needles with 0.1 mm diameter and 10:1 aspect ratio, and experiments of μIM and infrared-heating-assisted μIM are respectively carried out for comparison to verify the feasibility of the developed system.

3 Design of infrared heating device

3.1 Reflector

Reflector is the core component of the infrared heating device, whose role is to reflect the infrared energy to the heated surface with maximum efficiency. Reflector type and shape parameters directly influence the heating efficiency. For determining the shape of the reflector and achieving efficient infrared heating, the simulation of infrared heating efficiency on an

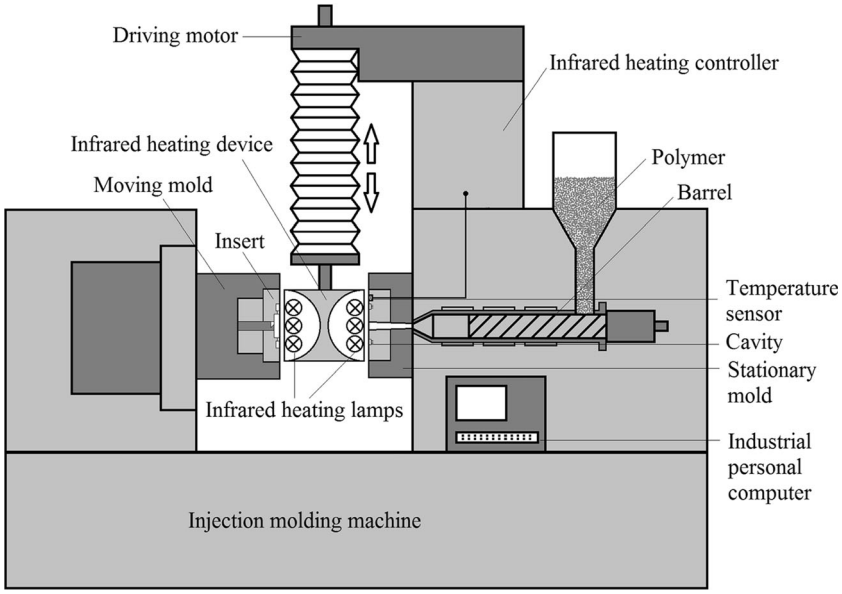

Fig. 1 The developed infrared-heating-assisted μIM system

insert surface is carried out. Several reflector types, which are common types of optical reflector for focus effect of infrared light and are easy to fabricate, including flat, spherical, rotating ellipsoidal, and rotating parabolic type, are selected and compared in the simulation. Some other reflector types are ignored because they cannot achieve focus effect or their reflection efficiency is not outstanding while their processing difficulties are significantly increased. In order to ensure the insert is covered, the room is enough for lamps and the heating efficiency could be compared; in this simulation, the lamps are gathered at the center point of the reflector bottom circle, and the length between the vertexes and the center points of flat, spherical, rotating ellipsoidal, and rotating parabolic types is 50 mm. The reflector types of infrared heating lamps are shown in Fig. 2. On the *y*-axis, the ordinate value "50" to "−50" represents the position on the insert, the value "30" to "−30" represents the position of runner and core, where the "effective heated region" can be defined as shown in Fig. 2 and requires high mold temperature for better melt fluidity, and the values "20" to "25" and "−20" to "−25" represent the position of the micro-needle array cavity in this research, where both high mold temperature and uniform temperature field are require for achieving a uniform flow speed and viscosity field without mutation.

The reflector surface is plated on a layer of aluminum in order to improve the infrared reflectivity. In the simulation, the reflectivity and the absorption rate of the aluminum film are 95 and 5%, respectively; the reflectivity and the absorption rate of the insert surface (polished #50 steel) are 55 and 45%, respectively. The initial temperature of the simulation environment is 20 °C, the power of each infrared heating lamps is 1000 W, and the duration of the radiation heating is 25 s. The temperature distribution on the insert surface is shown in Fig. 3.

The temperature distribution curves obtained by simulations are shown in Fig. 4. Although the temperature variation in the different mold positions corresponding to the different reflector types are somewhat different, all the temperature variation trends are the same. The temperature of the central point is the highest and the temperature of two sides decreases gradually. Simulated temperature data are shown in Table 2; the highest temperature of the central point is 175.1 °C achieved by the spherical reflector type, which means a lowest viscosity, highest melt flow speed, and best filling capability of the polymer melt in the runner. In the position of cavity, the reflector in spherical type, whose maximum temperature is 168.1 °C and temperature difference is 6.0 °C, achieves the highest and most uniform temperature in the micro-cavity.

Table 1 Process parameters of μIM process

Melt temperature (°C)	Mold temperature (°C)	Injection speed (mm/s)	Packing pressure (MPa)	Cooling time (s)	Packing time (s)
220	50	60	60	100	25

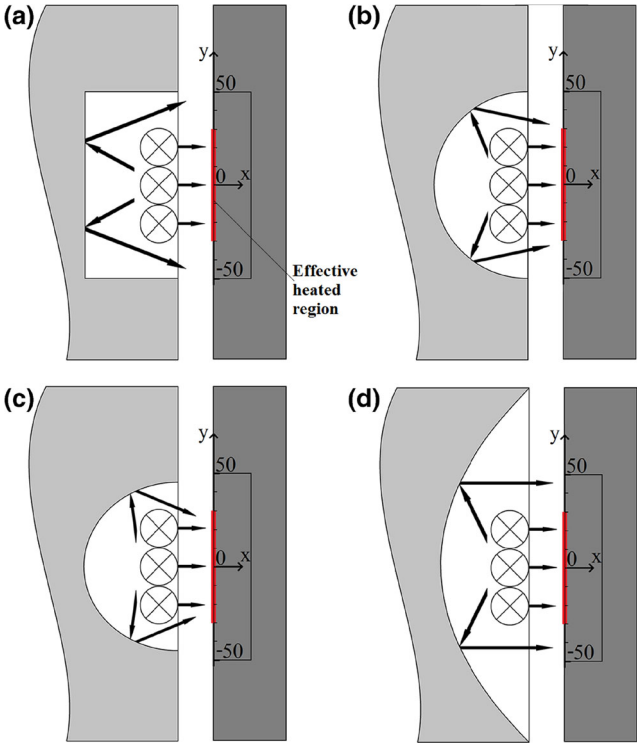

Fig. 2 The simulated reflector type of infrared heating lamps. **a** Flat type. **b** Spherical type. **c** Rotating ellipsoidal type. **d** Rotating parabolic type

This high and uniform temperature could reduce uneven shrinkage, and the high local temperature could avoid short shot during μIM. Furthermore, the spherical reflector results in a smallest temperature difference in the effective heated region that should afford a uniform flow performance in injection stage and a better fluidity of the polymer melt in packing stage. As the temperature distribution trends are the same, the spherical reflector, by which the temperature of the central point is the highest and the temperature in the region of the cavity is highest and most uniform, is determined to be the reflector type of the infrared heating device.

The radius of the spherical reflector has a great effect on the reflection efficiency. As the sphere has been determined to be the reflector type, a series of simulations of mold temperature are carried out in the same simulation condition to the above simulation, and the radius of the spherical reflector ranges

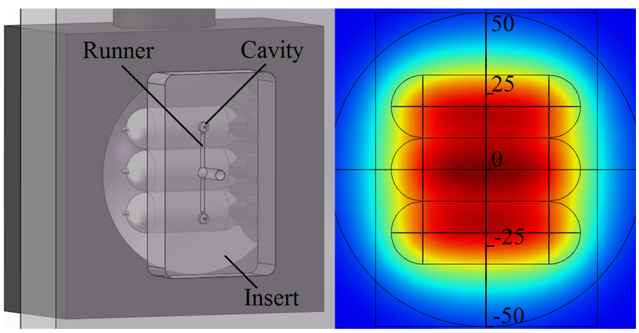

Fig. 3 The simulated temperature distribution on the insert surface

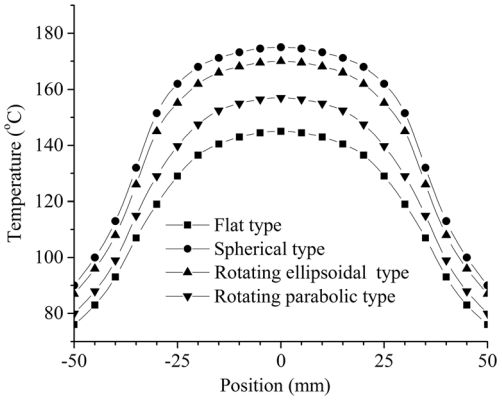

Fig. 4 Temperature distribution on the insert surface with different reflector types

from 30 to 70 mm, ensuring that the reflector could accommodate all lamps and properly cover the heated insert; the results are shown in Figs. 5 and 6. Figure 5 shows the central point temperature versus radius spherical reflectors. The temperature of the central point decreases with the increase of the radius of the spherical reflector. Figure 6 shows the temperature difference in the effective heated region of different radius spherical reflectors. The temperature difference quickly decreases with the increase of the radius of the spherical reflector when the radius is less than 50 mm. But once the radius is over 50 mm, the change of temperature difference becomes gentle. A high central point temperature and small temperature difference in the effective heated region mean better flow capability of the polymer melt in runner, better filling capability, and uniformity in micro-cavity, and this could achieve a uniform flow performance in injection stage and a better fluidity of the polymer melt in packing stage and subsequently achieve a

Table 2 Simulated temperature data of different reflector types

	Temperature of the central point (°C)	Maximum temperature in the cavity (°C)	Temperature difference in the cavity (°C)	Temperature difference in the effective heated region (°C)
Flat reflector type	145.8	136.2	7.5	26.8
Spherical reflector type	175.1	168.1	6.0	23.6
Rotating ellipsoidal reflector type	170.3	161.8	6.8	25.3
Rotating parabolic reflector type	157.2	147.5	7.7	28.2

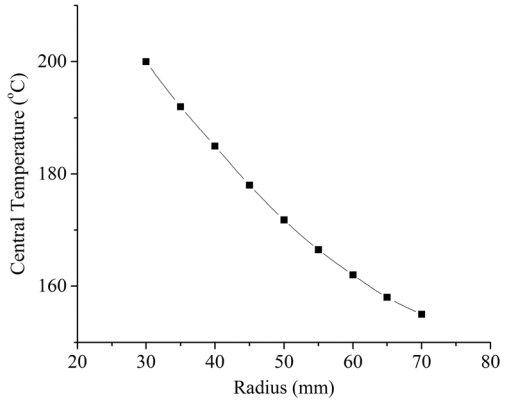

Fig. 5 Central point temperature of sphere types with different radius

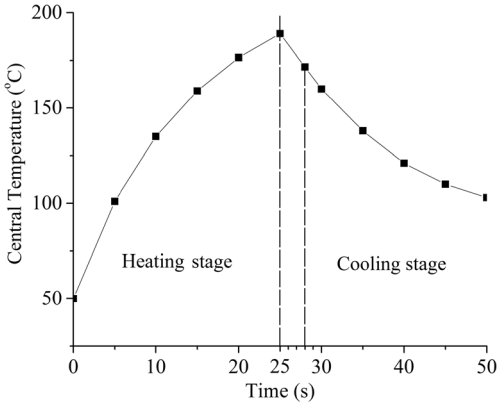

Fig. 7 The mold central point temperature variation

better mold filling quality and a lower shrinkage. Therefore, a spherical reflector with the radius of 50 mm is selected in order to ensure that the heating efficiency is as high as possible and, more importantly, to ensure that the temperature is uniform in the effective heated region to achieve a consistent quality of μIM.

Generally, the mold temperature is expected to be higher than the melting point of the selected crystalline polymer to ensure the fluidity of the melt. In this paper, PP is selected as the material, and the target mold temperature should be higher than 165 °C, which is the melting point of PP. However, before injection, the mold temperature will decrease because of the removal of the infrared heating device and the mold-closing, which take about 3 s in this research. Therefore, a numerical simulation is carried out to estimate the mold temperature at the beginning of injection, and the initial mold temperature is set as 50 °C because the mold is practically heated by the mold temperature controller. The mold central point temperature variation is shown in Fig. 7. It can be seen that the mold temperature dropped to 171.6 °C at the beginning of injection, which means that the mold heated by the designed infrared heating device can reach the target temperature, although a certain temperature decrease occurred during the removal of the infrared heating device and the mold-closing.

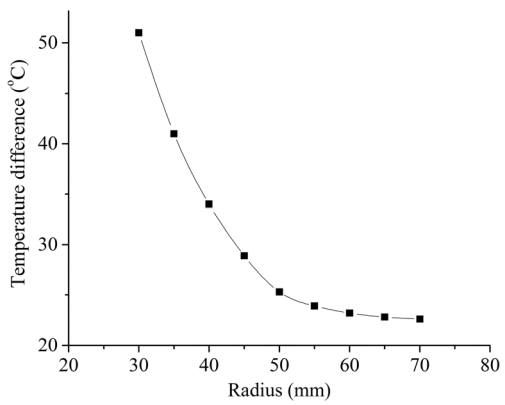

Fig. 6 Temperature difference in effective heated region of sphere types with different radius

3.2 Heating experiment

A verification experiment is done to verify the validity of the designed infrared heating device. An insert (150 × 100 × 20 mm, polished #50 steel) is heated by the infrared heating device. Ten holes are drilled on the reverse side of the heated metal surface for installing the temperature sensors in order to measure the temperature distribution and changing trend of the heated metal surface, each hole with a diameter of 1.5 mm and 19 mm deep. The temperature measuring schematics are shown in Fig. 8. Hole 1 is located in the center of the insert, Hole 1 to Hole 7 are the position of runner and cavity, and Hole 7 to Hole 10 are the periphery of the cavity.

The initial temperatures of environment is 20 °C before heating, and the heating time is 25 s. The temperature distribution after heating is shown in Fig. 9; the temperature of Hole 1 increased from 19.96 to 174.14 °C in 25 s. Compared with the simulation result which is the temperature distribution curve of spherical reflector in Fig. 4, the experimental result has the same distribution trend and a few deviations in value. This deviation is mainly caused by the difference between the simulated ideal model and actual situation in the aspect of the structure and dimension of the heated mold, material parameters of the heated surface, the air flow in the experimental environment, and so on. The temperature difference between Hole 1 and Hole 7 located in the effective heated region defined in the simulation is 25.11 °C, the temperature difference between Hole 5 and Hole 6, which is the position of the micro-needle array cavity, is 5.46 °C, while the temperature drop from Hole 7 to Hole 10 outside the effective heated region is relatively larger, which can reach 49.85 °C. The temperature threshold in the infrared heating control system is set according to the position of the temperature sensor in the insert and the corresponding expected temperature value which is obtained from the result of the heating experiment. The small temperature difference in the effective heated region and more importantly in the micro-cavity means a uniform enough mold temperature field which could achieve a

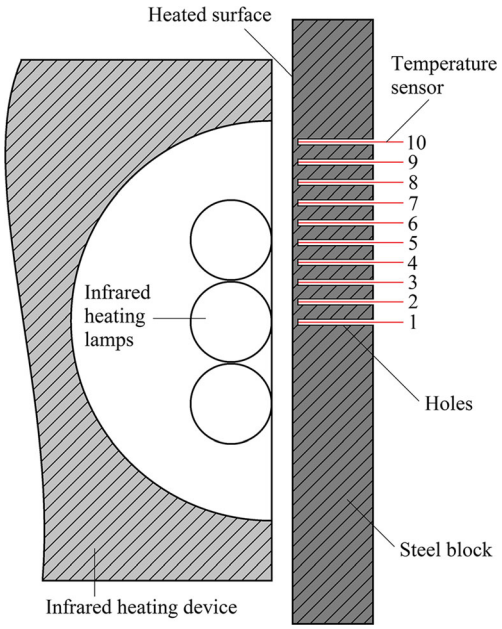

Fig. 8 Diagram of temperature measurement

uniform flow speed and viscosity field without mutation and avoid uneven shrinkage and short shot.

During the heating process, the temperatures are measured by temperature sensors and sent to the computer in real time. The heating stage is 0 to 25 s, and then heating stops and cooling stage begins. The temperature curves of the temperature measurements in Hole 1 to Hole 7 are shown in Fig. 10, T_1 to T_7 are the temperatures in Hole 1 to Hole 7, respectively, and the results show that the heating and cooling stages of different measurement holes are synchronous without high temperature gradient in the mold. This synchronous heating and cooling stages of the mold could provide a uniform melt temperature field before and during injection molding.

The validity of this designed infrared heating device is verified by the above heating experiment. The experimental results are in agreement with the simulation data, indicating that this new infrared heating device can cover the melt flow area completely and achieve uniform heating. Uniform mold

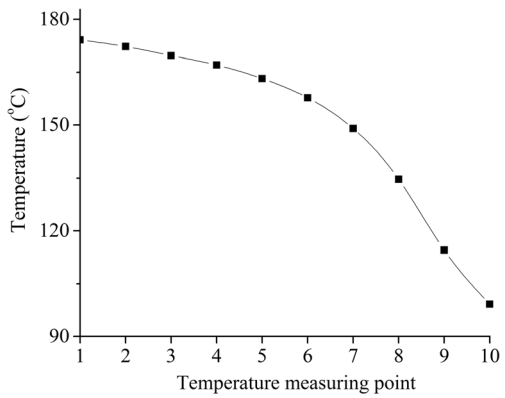

Fig. 9 Temperature distribution after heating 25 s

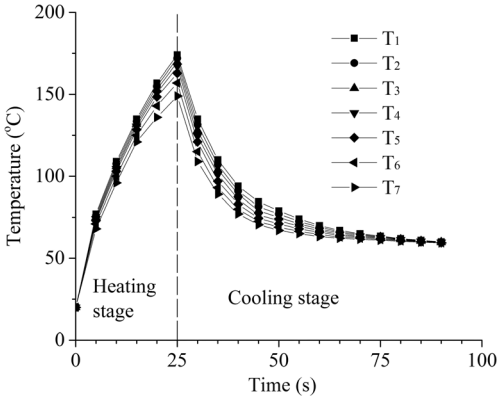

Fig. 10 Temperature curves of Hole 1 to Hole 7

temperature field could achieve a uniform flow speed and viscosity field without mutation, and then molding defects such as uneven shrinkage and short shot are avoided. Thus, the designed infrared heating device could be used in the developed infrared-heating-assisted μIM system.

4 Results and discussion

An infrared-heating-assisted μIM experiment for fabricating micro-needle array is carried out to clarify the influence on mold filling quality (such as the height and the radial shrinkage). The fabricated micro-needle arrays are shown in Fig. 11; the height and uniformity of needles, measured by a digital microscope, are increased by the assistance of infrared heating. In each experiment, five simple parts are randomly measured and analyzed in order to comprehend which aspect of the developed system is beneficial for the improvement of micro-needle array quality. The statistics of micro-needle heights (h_{ij}) is shown in Table 3; with the assistance of infrared heating, the average of mean height ($\overline{\mu_{h_{ij}}}$) is increased from 591.27 to 802.81 μm, and the rate of increase is 35.78%. Moreover, the average of standard deviation ($\overline{\sigma_{h_{ij}}}$) is decreased from 238.13 to 127.92 μm, and the rate of decrease is 46.28%. The mean height and uniformity of the micro-needles which are fabricated by the developed infrared-heating-assisted μIM system are significantly improved.

When flowing in runner and cavity, the melt is going through a process of cooling by the mold, and especially in micro-cavity with high aspect ratio, the cooling is more rapid and less uniform. While the mold temperature is raised by infrared heating device, the melt temperature in the cavity becomes higher and the distribution of temperature is also more uniform, which makes the flow performance of the polymer melt better during infrared-heating-assisted μIM process and leads to higher and more uniform micro-needles as the results have shown.

During the injection molding process, high shrinkage is one of the biggest challenges which deteriorate the quality of

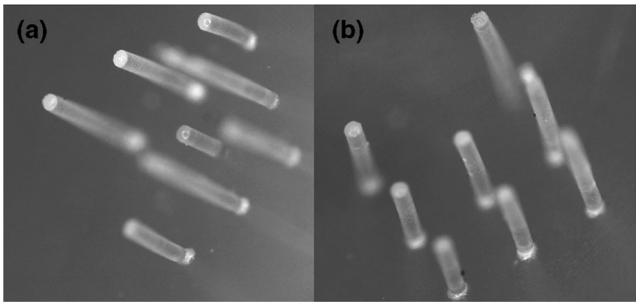

Fig. 11 Micro-needle array **a** fabricated by μIM and **b** fabricated by infrared-heating-assisted μIM

produced parts and could be influenced by melt temperature. During this process, because of the temperature decrease and the crystallization (if it exists), the density of the polymer will increase. After the cavity is filled, the compensation of material shrinkage should be realized by means of pressuring on the cavity through the packing stage. In general, the increase in mold temperature could lead to low viscosity of the polymer melt, increased pressure delivered to the cavity, and prolonged sealing time of the gate, and these are beneficial for shrinkage compensation which could result in a lower and uniform shrinkage. As the developed method could achieve improvement of micro-needle height by increasing the mold temperature, the influence of infrared heating on shrinkage in this method should be determined.

The statistics of micro-needle radial shrinkage (s_{ij}) is shown in Table 4. With the assistance of infrared heating, the average of mean shrinkage ($\overline{\mu_{s_i}}$) is decreased from 0.89 to 0.78%, and the rate of decrease is 12.4%; at the same time, the average of standard deviation (σ_{s_i}) is increased from 0.96 to 0.98%, and the rate of increase is 2.08%. It shows that the infrared heating is beneficial for the mean shrinkage of micro-needles, besides making the shrinkage more uneven. During the infrared-heating-assisted μIM of micro-needle array, the cooling time of the PP part increases with the increase of the mold temperature, which means that the temperature range of high crystallization rate is longer and the crystallinity of the PP part increased which could result in a higher and uneven shrinkage. The shrinkage is affected by the comprehensive effect of the decreased shrinkage by increased packing compensation and the increased shrinkage by increased crystallinity of PP part, and the increased packing compensation relatively plays a more important role in the influence on shrinkage in this method.

Based on the statistics and analysis of micro-needle height and shrinkage, the feasibility of the developed infrared-heating-assisted μIM system is clarified. With the assistance of infrared heating, the flow performance of polymer melt is improved, which means a higher and more uniform filling capability of melt in micro-cavity with high aspect ratio.

5 Conclusions

This paper focused on the feasibility of the developed infrared-heating-assisted μIM system on improving molding quality of micro-needle array. An infrared heating device with high efficiency was designed to rapidly raise the mold temperature, and influences of reflector types on the mold temperature were discussed. A μIM experiment for fabricating micro-needle array was carried out by the developed infrared-heating-assisted device. The experiment results showed that the surface temperature of the insert was raised from 19.96 to 174.14 °C within 25 s; meanwhile, the effective heated region was covered by the infrared system radiation area, and the temperature difference in the area of cavity was 5.46 °C, which meant a uniform temperature field was formed in the micro-cavity. Based on the analysis and discussion of the micro-needle array injection molding experimental results, the average of mean height was increased by 35.78%, and the average of standard deviation was decreased by 46.28% and the micro-needle height increased and became uniform by the assistance of infrared heating. The average of mean shrinkage was decreased by 12.4%, the average of standard deviation increased by 2.08%, the shrinkage of micro-needles was decreased, and the increased packing compensation played a more important role in the influence on shrinkage than the increased crystallinity of PP part. The feasibility of the developed infrared-heating-assisted μIM system was verified by the improved filling height, uniformity, and shrinkage of micro-needle arrays.

Table 3 Statistical table of micro-needle heights

	μIM	Infrared-heating-assisted μIM
Mean height (μ_{h_i}, μm)[a]	608.67, 637.41, 569.70, 571.12, 569.44	794.56, 825.41, 816.76, 791.24, 786.09
Average of mean height ($\overline{\mu_{h_i}}$, μm)[b]	591.27	802.81
Standard deviation (σ_{h_i}, μm)[c]	218.41, 269.29, 226.16, 233.50, 243.31	116.11, 112.62, 140.51, 144.20, 126.18
Average of standard deviation ($\overline{\sigma_{h_i}}$, μm)[d]	238.13	127.92

[a] $\mu_{h_i} = \frac{1}{8}\sum_{j=1}^{8} h_{ij}$; [b] $\overline{\mu_{h_i}} = \frac{1}{5}\sum_{i=1}^{5}\mu_{h_i}$; [c] $\sigma_{h_i} = \sqrt{\frac{1}{8}\left(\sum_{j=1}^{8}\left(h_{ij}-\mu_{h_i}\right)^2\right.}$; [d] $\overline{\sigma_{h_i}} = \frac{1}{5}\sum_{i=1}^{5}\sigma_{h_i}$

Table 4 Statistical table of micro-needle shrinkage

	μIM	Infrared-heating-assisted μIM
Mean shrinkage (μ_{s_i}, %)[e]	0.67, 0.97, 0.64, 1.14, 1.01	1.11, 0.90, 0.56, 0.62, 0.72
Average of mean height ($\overline{\mu_{s_i}}$, %)[f]	0.89	0.78
Standard deviation (σ_{s_i}, %)[g]	1.23, 0.74, 1.31, 0.71, 0.80	0.79, 1.04, 0.76, 1.15, 1.14
Average of standard deviation ($\overline{\sigma_{s_i}}$, %)[h]	0.96	0.98

[e] $\mu_{s_i} = \frac{1}{8}\sum_{j=1}^{8} s_{ij}$; [f] $\overline{\mu_{s_i}} = \frac{1}{5}\sum_{i=1}^{5}\mu_{s_i}$; [g] $\sigma_{s_i} = \sqrt{\frac{1}{8}\left(\sum_{j=1}^{8}\left(s_{ij}-\mu_{s_i}\right)^2\right)}$; [h] $\overline{\sigma_{s_i}} = \frac{1}{5}\sum_{i=1}^{5}\sigma_{s_i}$

Acknowledgements The authors would like to thank the National Natural Science Foundation of China (no. 51375336) and Key Program of Tianjin Municipal National Natural Science of China (no. 12JCZDJC27900) for the financial support.

References

1. Prausnitz MR (2004) Microneedles for transdermal drug delivery. Adv Drug Deliv Rev 56(5):581–587
2. Goncalves SB, Oliveira MJ, Peixoto AC, Silva AF, Correia JH (2016) Out-of-plane neural microelectrode arrays fabrication using conventional blade dicing. Int J Adv Manuf Technol 85(1):431–442
3. Michaeli W, Opfermann D, Kamps T (2007) Advances in micro assembly injection moulding for use in medical systems. Int J Adv Manuf Technol 33(1):206–211
4. Oh J, Liu K, Medina T, Kralick F, Noh H (2014) A novel microneedle array for the treatment of hydrocephalus. Microsyst Technol 20(6):1169–1179
5. Wang MH, Zhu D (2009) Fabrication of multiple electrodes and their application for micro-holes array in ECM. Int J Adv Manuf Technol 41(1):42–47
6. Park IB, Ha YM, Lee SH (2010) Cross-section segmentation for improving the shape accuracy of microstructure array in projection microstereolithography. Int J Adv Manuf Technol 46(1):151–161
7. Li K, Ju J, Xue Z, Ma J, Feng L, Gao S, Jiang L (2013) Structured cone arrays for continuous and effective collection of micron-sized oil droplets from water. Nat Commun 4(4):2276–2276
8. Valdés-Ramírez G, Li YC, Kim J, Jia W, Bandodkar AJ, Nuñez-Flores R, Miller PR, Wu SY, Narayan R, Windmiller JR, Polsky R, Wang J (2014) Microneedle-based self-powered glucose sensor. Electrochem Commun 47:58–62
9. Forvi E, Bedoni M, Carabalona R, Soncini M, Mazzoleni P, Rizzo F, O'Mahony C, Morasso C, Cassarà DG, Gramatica F (2012) Preliminary technological assessment of microneedles-based dry electrodes for biopotential monitoring in clinical examinations. Sens Actuators A 180(180):177–186
10. Zhou W, Song R, Pan X, Peng Y, Qi X, Peng J, Hui KS, Hui KN (2013) Fabrication and impedance measurement of novel metal dry bioelectrode. Sens Actuators A 201(10):127–133
11. Jiang BY, Zhou MY, Weng C, Zhang L, Lv H (2016) Fabrication of nanopillar arrays by combining electroforming and injection molding. Int J Adv Manuf Technol 86(5–8):1319–1328
12. Lu Z, Zhang KF (2009) Morphology and mechanical properties of polypropylene micro-arrays by micro-injection molding. Int J Adv Manuf Technol 40(5):490–496
13. Sha B, Dimov S, Griffiths C, Packianather MS (2007) Micro-injection moulding: factors affecting the achievable aspect ratios. Int J Adv Manuf Technol 33(1–2):147–156
14. Kim WW, Gang MG, Min BK, Kim WB (2014) Experimental and numerical investigations of cavity filling process in injection moulding for microcantilever structures. Int J Adv Manuf Technol 75(1–4):293–304
15. Qiu Z, Zheng H, Fang FZ, Wang HY (2012) Longitudinal ultrasound-assisted micro-injection moulding method. Nanotechnol Precis Eng 10(2):170–176
16. Gao S, Qiu Z, Ma Z, Yang Y (2016) Flow properties of polymer melt in longitudinal ultrasonic-assisted micro-injection molding. Polym Eng Sci. doi:10.1002/pen.24455
17. Qiu Z, Yang X, Zheng H, Gao S, Fang F (2015) Investigation of micro-injection molding based on longitudinal ultrasonic vibration core. Appl Opt 54(28):8399–8405
18. Attia UM, Alcock JR (2010) Optimising process conditions for multiple quality criteria in micro-injection moulding. Int J Adv Manuf Technol 50(5):533–542
19. Kurt M, Kaynak Y, Kamber OS, Mutlu B, Bakir B, Koklu U (2010) Influence of molding conditions on the shrinkage and roundness of injection molded parts. Int J Adv Manuf Technol 46(5):571–578
20. Chen SC, Peng HS, Chang JA, Jong WR (2004) Simulations and verifications of induction heating on a mold plate. Int Commun Heat Mass Transfer 31(7):971–980
21. Kim DH, Kang MH, Chun YH (2001) Development of a new injection molding technology: momentary mold surface heating process. J Injection Molding Technol 5(4):229–232
22. Xiao CL, Huang HX (2014) Development of a rapid thermal cycling molding with electric heating and water impingement cooling for injection molding applications. Appl Therm Eng 73(1):710–720
23. Jeng MC, Chen SC, Minh PS, Chang JA, Chung CS (2010) Rapid mold temperature control in injection molding by using steam heating. Int Commun Heat Mass Transfer 37(9):1295–1304
24. Chang PC, Hwang SJ (2006) Experimental investigation of infrared rapid surface heating for injection molding. J Appl Polym Sci 102(4):3704–3713
25. Chang PC, Hwang SJ (2006) Simulation of infrared rapid surface heating for injection molding. Int Commun Heat Mass Transfer 49(21–22):3846–3854
26. Saito T, Satoh I, Kurosaki Y (2002) A new concept of active temperature control for an injection molding process using infrared radiation heating. Polym Eng Sci 42(12):2418–2429
27. Yu MC, Young WB, Hsu PM (2007) Micro-injection molding with the infrared assisted mold heating system. Mater Sci Eng A 460(14):288–295